ADVANCED FUNCTIONAL MATERIALS
www.afm-journal.de

Pushing the Cycling Stability Limit of Polypyrrole for Supercapacitors

Yu Song, Tian-Yu Liu, Xin-Xin Xu, Dong-Yang Feng, Yat Li, and Xiao-Xia Liu**

Polypyrrole (PPy) is a promising pseudocapacitive material for supercapacitor electrodes. However, its poor cycling stability is the major hurdle for its practical applications. Here a two-prong strategy is demonstrated to stabilize PPy film by growing it on a functionalized partial-exfoliated graphite (FEG) substrate and doping it with β-naphthalene sulfonate anions (NS^-). The PPy electrode achieves a remarkable capacitance retention rate of 97.5% after cycling between –0.8 and 0 V versus saturated calomel electrode for 10 000 cycles. Moreover, an asymmetric pseudocapacitor using the stabilized PPy film as anode also retains 97% of capacitance after 10 000 cycles, which is the best value reported for PPy-based supercapacitors. The exceptional stability of PPy electrode can be attributed to two factors: 1) the flexible nature of FEG substrate accommodates large volumetric deformation and 2) the presence of immobile NS^- dopants suppresses the counterion drain effect during charge–discharge cycling.

1. Introduction

Polypyrrole (PPy) is a promising pseudocapacitor electrode material due to its low cost, low environmental toxicity, high electrical conductivity (≈100–10 000 S m^{-1}), wide potential window, and ease of fabrication.[1–5] However, these advantages are offset by its very poor cycling stability (usually <50% capacitance retention after 1000 charge–discharge cycles in aqueous electrolytes).[1,2,6,7] The charge/discharge cycling instability of PPy is mainly due to structural pulverization and counterion drain effect.[1,2,6,8] Upon oxidation, positive charged nitrogen groups (polarons) are generated on PPy chains. To balance the charge, counterions in the electrolyte will diffuse into the backbone of PPy chains, causing PPy to swell. Upon reduction, polarons are neutralized by the injected electrons. Meanwhile, counterions diffuse back into electrolyte in order to maintain the neutrality of the PPy matrix, which subsequently causes PPy backbone to shrink.[8–10] The repeated swelling and shrinking of PPy chains leads to structural pulverization, resulting in activity loss. Moreover, PPy also suffers from counterion drain effect, *i.e.*, less and less anions can dope into the PPy matrix after repeated charge and discharge cycling due to the irreversible insertion/extrusion of counterions.[4,6,9–11] For instance, when anions diffuse back into electrolyte during reduction, some of the ion channels of PPy will collapse and form a compact structure. Re-oxidation of the PPy chains requires extra energy to re-open the compact structure,[6] making anions more difficult to redope the PPy backbone. As a result, less polarons can be regenerated. Since the electrical conductivity of PPy is directly proportional to the number of polarons on the backbone of PPy chains,[10] the counterion drain effect will slowly reduce the electrical conductivity of PPy, and hence, the capacitance.

Enormous efforts have been made to stabilize PPy-based materials for pseudocapacitors.[1,3,4,12–16] One of the strategies is integrating PPy into flexible substrates/current collectors such as reduced graphene oxide (rGO)[13,14,17] and carbon nanotubes (CNT).[18] Flexible substrates can accommodate large volumetric change of PPy during charge and discharge, and thus, effectively suppress structural pulverization of PPy. Our previous work showed that PPy anchored on partially exfoliated graphene substrate retained as high as 91% of its initial capacitance after 1000 cycles in 3 M KCl aqueous electrolyte.[2] Another strategy is to dope PPy with special anionic dopants. For example, PPy doped with Tiron[15] and sulfanilic acid azochromotrop[16] achieved excellent capacitance retention rate of 93.1% and 91.5% after 1000 charge–discharge cycles, respectively. It was believed that the hydroxyl groups in the dopants behave as chelating agents and form dative covalent bonds with the Ni current collector, thus improving adhesion of PPy film.[15,16] However, the stability of these PPy electrodes is still far below the satisfactory level for commercial applications. And there is no report on how to simultaneously address the structural pulverization and counterion drain effect.

Here we demonstrate for the first time to improve the cycling stability of PPy by addressing both the structural pulverization and counterion drain effect. A functionalized partial-exfoliated graphite substrate (FEG) was synthesized by a two-step partial exfoliation method reported previously.[19] We deposit PPy onto FEG substrate, and simultaneously dope the PPy film by β-naphthalene sulfonate anions (NS^-) with high steric hindrance and low mobility[20] within the polymer matric

Y. Song, Prof. X.-X. Xu, D.-Y. Feng, Prof. X.-X. Liu
Department of Chemistry
Northeastern University
Shenyang 110819, P. R. China
E-mail: xxliu@mail.neu.edu.cn
T.-Y. Liu, Prof. Y. Li
Department of Chemistry and Biochemistry
University of California-Santa Cruz
1156 High Street, Santa Cruz, CA 95064, USA
E-mail: yatli@ucsc.edu

DOI: 10.1002/adfm.201501709

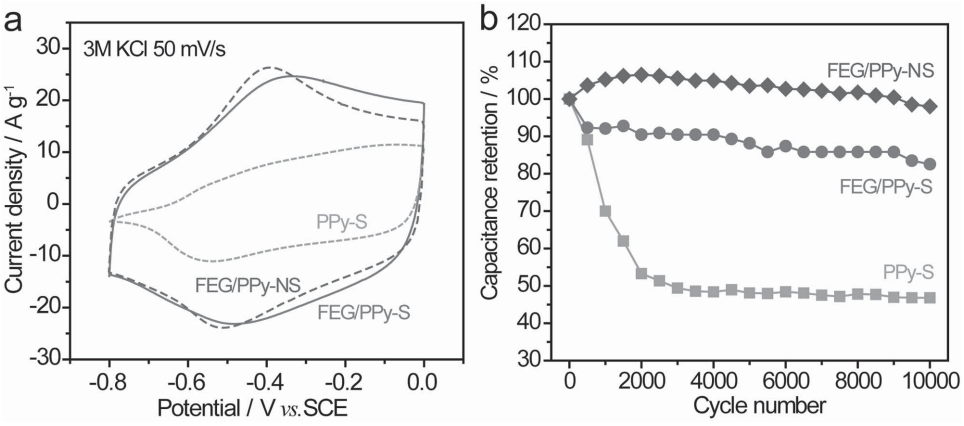

Figure 1. a) Cyclic voltammograms of PPy-S, FEG/PPy-S, and FEG/PPy-NS collected at a scan rate of 50 mV s^{-1} in 3 M KCl electrolyte solution. b) Electrochemical cycling stability of PPy-S, FEG/PPy-S, and FEG/PPy-NS measured by galvanostatic charge/discharge cycling between –0.8 and 0 V versus SCE at a current density of 4 mA cm^{-2} in 3 M KCl electrolyte solution.

to suppress counterion drain effect. The electrode exhibited excellent cycling stability with 97.5% capacitance retention after 10 000 consecutive charge–discharge cycles in a negative potential window between 0 and –0.8 V versus saturated calomel electrode (SCE). Moreover, an asymmetric pseudocapacitor device composed of the stabilized PPy anode and FEG supported MnO_2 nanosheet (FEG/MnO_2) cathode showed remarkable cycling stability with only 3% capacitance loss after 10 000 cycles. To our knowledge, this is the best capacitance retention rate ever achieved for PPy-based pseudocapacitor devices.

2. Results and Discussion

2.1. Improvement of Cycling Stability of PPy Film

The electrochemical performance of the three electrodes was tested in a three-electrode system. As shown in **Figure 1**a, all three electrodes exhibited a pair of broad redox peaks corresponding to pseudocapacitive reactions (insertion and extrusion of counterions).[21,22] The FEG/PPy-NS and FEG/PPy-S electrodes have comparable pseudocapacitive behavior, rate capability (Figure S2, Supporting Information), and specific capacitances (338 F g^{-1} and 326 F g^{-1}@ 50 mV s^{-1}, respectively). Their specific capacitances are substantially higher than that of PPy-S (130 F g^{-1}@ 50 mV s^{-1}). The enhanced capacitance of FEG/PPy-S and FEG/PPy-NS can be ascribed to the increased surface area after electrochemical treatment of graphite foil[19] (Figure S3, Supporting Information). While the addition of NS^- doping has limited effect on the capacitance of PPy film, it significantly improves the cycling stability of PPy film. Figure 1b compares the electrochemical cycling stability of the three electrodes tested by galvanostatic charge/discharge cycling method for 10 000 cycles. FEG/PPy-NS showed the best cycling stability with an excellent capacitance retention rate of 97.5% after 10 000 cycles. The initial increase in capacitance is believed to be due to the electro-activation process.[3] On the contrary, the FEG/PPy-S and PPy-S electrodes only retained 82.6% and 46.8% of their initial capacitances, respectively.

2.2. Mechanism of Stability Enhancement

To understand the possible mechanisms leading to the exceptional stability of FEG/PPy-NS electrode, we performed the following experiments. First, scanning electron microscopy (SEM) images were collected for the three electrodes before and after the cycling test. PPy-S film on graphite foil showed many cracks and started to peel off from the substrate after testing for 10 000 cycles (**Figure 2**a). These cracks were formed as a result of structural pulverization due to the repeated volumetric swelling and shrinking. It correlates with the rapid capacitance degradation of PPy-S. By contrast, the morphology of FEG/PPy-S and FEG/PPy-NS electrodes remained unchanged after 10 000 cycles. The enhanced cycling stability can be ascribed to the mechanically flexible nature of the FEG substrate. It has been reported that flexible substrates can accommodate large volumetric expansion and so alleviate structural pulverization and improve the stability of PPy.[1,18,22,23] Furthermore, the film thickness may also affect the cycling stability of PPy film. To test this hypothesis, PPy-S electrode with reduced film thickness (≈150–200 nm, comparable to the film thickness of FEG/PPy-S and FEG/PPy-NS) was prepared in the same conditions as other PPy-S electrodes except the electrodeposition time was reduced from 15 to 2 min. As shown in Figure S4 (Supporting Information), the PPy-S electrode with reduced film thickness indeed exhibits improved cycling stability compared to the electrode with thick PPy-S film, with capacitance retention of 76.5% after 10 000 cycles. While this value is still smaller than the capacitance retention rate of PPy-NS film (97.5%) or PPy-S film (82.6%) supported on FEG, the results suggest that reducing PPy film thickness is beneficial for improving its cycling stability. However, the improved stability of PPy-S electrode with reduced film thickness on graphite foil is at the cost of mass loading. Using FEG substrate with large surface area and flexibility is more favorable because it can improve the cycling stability of PPy electrode with higher mass loading.

To explain the difference of cycling stability between FEG/PPy-NS and FEG/PPy-S samples, we further collected energy-dispersive spectroscopy (EDS) and X-ray photoelectron spectroscopy (XPS) spectra for the two electrodes. Both EDS

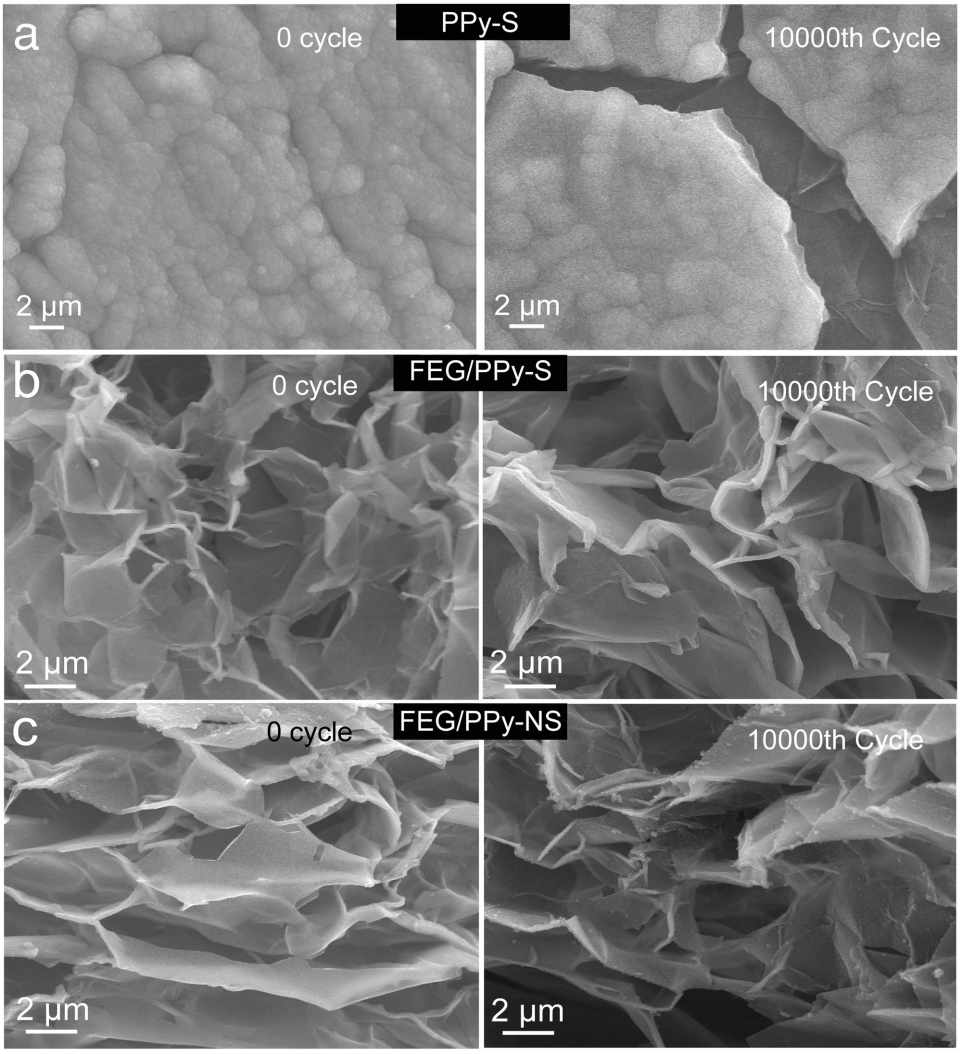

Figure 2. SEM images of a) PPy-S, b) FEG/PPy-S, and c) FEG/PPy-NS collected before and after testing 10 000 cycles.

(**Figure 3**a) and XPS (Figure S5, Supporting Information) data confirm the presence of S signal in both sample before cycling test, suggesting the successful doping of sulfate ions into the FEG/PPy-S electrode and NS^- into the FEG/PPy-NS electrode. Notably, the S signal of FEG/PPy-S almost disappeared after testing for 10 000 cycles. This is believed to be due to the loss of sulfate ions caused by the counterion drain effect, which is consistent with the previous reports on PPy electrodes.[6,8,21] On the contrary, there was no obvious decay of S signal in the FEG/PPy-NS sample after cycling stability test (Figure 3b). Apparently the introduction of NS^- doping can minimize the counterion drain effect, which has never been reported before. It is known that the mobility of anions in PPy structure is inversely proportional to their sizes.[21] In comparison to sulfate ions, we believe that NS^- anions are less likely to leave the backbone of PPy chain during redox processes due to its large molecular size and the strong π–π interactions between benzene rings of NS^- and pyrrole rings of PPy. As a result, the NS^- doped PPy suppresses counterion drain effect and retains excellent electrical conductivity during cycling test, and hence, the excellent capacitance retention rate.

We carried out XPS experiments to test our hypothesis. Figure 3c,d show the N 1s core level spectra collected for FEG/PPy-S and FEG/PPy-NS samples before and after the cycling test. Before cycling, the N 1s core level spectra of both sample can be deconvoluted into two synthetic Gaussian peaks centered at 398.3 and 399.8 eV, respectively, corresponding to —N= and —NH— nitrogen atoms in the backbone of PPy chain.[2] The high binding energy tail over 400 eV indicates the presence of polarons (—N^+= and —N^+H— cations).[2,14,24] The synthetic peaks centered at 401.8 and 402.2 eV can be assigned to —N^+H— cations and —N^+= cations, respectively. After cycling, as shown in Figure 3c, the FEG/PPy-S electrode showed less pronounced high energy tail and much higher —N= signal. The increased amount of —N= is consistent with the previous report that PPy polarons can be reduced to —N= during reduction.[24] The polaron ratio, defined as the areal ratio between the polaron signals (—N^+= and —N^+H— peaks) and the total nitrogen signal (—N^+=, —N^+H—, —NH—, and

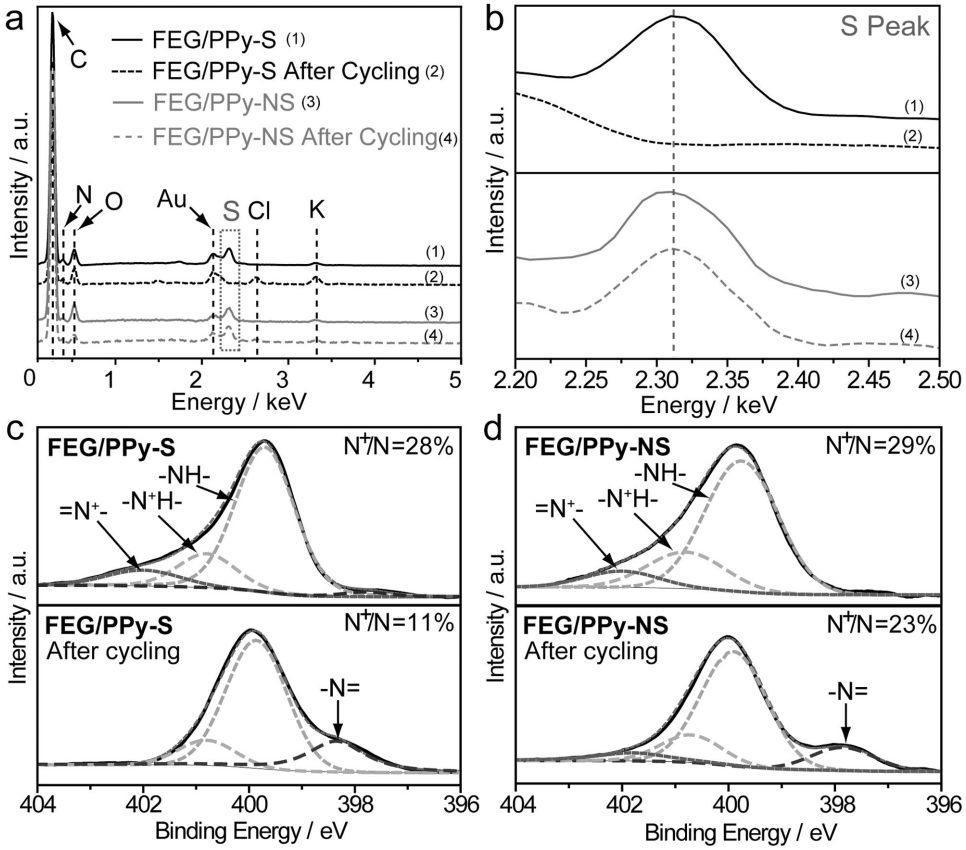

Figure 3. a) EDS spectra and b) S peak signal collected for FEG/PPy-S and FEG/PPy-NS before and after cycling test. N 1s spectra of c) FEG/PPy-S and d) FEG/PPy-NS before and after cycling test.

—N= peaks), decreased drastically from 28% to 11%. By contrast, the polaron ratio of FEG/PPy-NS only experienced a small decay from 29% to 23% as less of the —N^+= cations were converted to —N=. Additionally, C 1s XPS spectra collected for FEG/PPy-S and FEG/PPy-NS before and after the cycling test are comparable (Figure S6, Supporting Information), indicating the PPy carbon backbone was stable during cycling. XPS results clearly showed that the FEG/PPy-S suffers from the substantial loss of polarons during cycling, while PPy doped with NS^- can effectively minimize the counterion drain effect and retain the amount of polarons. Furthermore, electrochemical impedance spectroscopy (EIS) data show that the charge transfer resistance of both PPy-S and FEG/PPy-S increased substantially after stability test (Figure S7, Supporting Information). This is consistent with our hypothesis that the ion doping and de-doping between electrolyte and electrode become more difficult as the electrical conductivity of electrode decreases with the increasing cycle number due to the counterion drain effect. FEG/PPy-NS, on the contrary, shows similar EIS profile and charge transfer resistance before and after the cycling stability test. The results again prove that NS^- doping can minimize counterion drain effect of PPy electrode. Taken together, these results explain clearly why FEG/PPy-NS has the best capacitance retention rate among the three electrodes.

2.3. Stability of the Asymmetric Pseudocapacitors Based on FEG/PPy-NS as Anode

The successful demonstration of stable PPy electrode can open up new opportunities for fabrication of pseudocapcitive devices. We assembled an asymmetric pseudocapacitor device using FEG/PPy-NS as anode and MnO_2 nanostructures supported on FEG substrate (FEG/MnO_2)[19] as cathode (Figure S8, Supporting Information). The device is denoted as FEG/PPy-NS//FEG-MnO_2. FEG/MnO_2 electrode shows excellent specific capacitance within a potential window of 0–1 V versus SCE (Figure S9a, Supporting Information). By coupling the FEG/MnO_2 cathode and FEG/PPy-NS anode, the asymmetric device exhibits a stable potential window up to 2 V. (Figure S9, Supporting Information).

Significantly, the asymmetric pseudocapacitor showed an exceptional electrochemical cycling stability with capacitive retention rate of 97% after testing for 10 000 galvanostatic charge/discharge cycles at the current density of 6 A g^{-1} (**Figure 4**a). Coulombic efficiency remains almost 100% at all cycles. The initially increased capacitance can be ascribed to the electro-activation process, which has been commonly observed for metal oxide based devices.[3,25] For comparison, the capacitance retention rates of FEG/PPy-S//FEG/MnO_2 and PPy-S//FEG/MnO_2 under the same test conditions were only

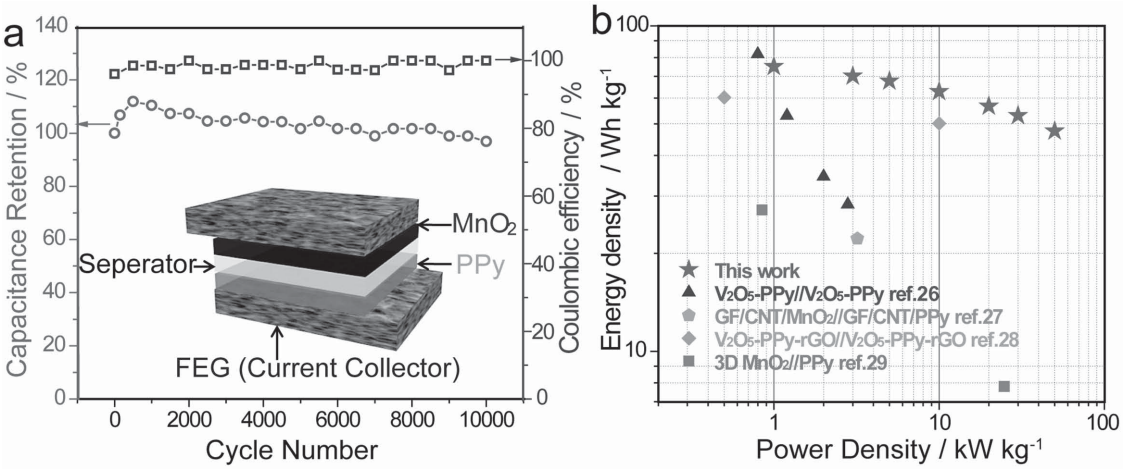

Figure 4. a) Cycling stability and coulombic efficiency of FEG/PPy-NS//FEG/MnO_2 pseudocapacitor measured by galvanostatic charge/discharge at a current density of 6 A g^{-1} in 3 M KCl aqueous electrolyte. Inset shows the schematic illustration of the FEG/PPy-NS//FEG/MnO_2 asymmetric pseudocapacitor. b) Ragone plot of FEG/PPy-NS//FEG/MnO_2 pseudocapacitor with other reported values for comparison.

78% and 46%, respectively (Figure S10, Supporting Information). It clearly shows that the stable PPy electrode is the key for achieving the outstanding device cycling stability. To our knowledge, the capacitance retention rate obtained from FEG/PPy-NS//FEG/MnO_2 device is the best value reported for PPy-based electrochemical capacitors (**Table 1**). Furthermore, the improved cycling stability is not at the price of electrochemical performance. As shown in Figure 4b, FEG/PPy-NS//FEG/MnO_2 device is able to deliver a maximum energy density of 75 W h kg^{-1} at power density of 1 kW kg^{-1} or 48 W h kg^{-1} at an ultra-high power density of 50 kW kg^{-1}. These values are among the best values reported for pseudocapacitor devices using PPy-based anode, such as V_2O_5-PPy//V_2O_5-PPy (53.5 W h kg^{-1} at 1.2 kW kg^{-1}),[26] GF/CNT/PPy//GF/CNT/MnO_2 (22.2 W h kg^{-1} at 3.2 kW kg^{-1}),[27] V_2O_5-PPy-rGO//V_2O_5-PPy-rGO (60.3 W h kg^{-1} at 0.5 kW kg^{-1}),[28] and PPy//3D MnO_2 (27.2 W h kg^{-1} at 0.85 kW kg^{-1}).[29]

3. Conclusion

We have demonstrated that the cycling stability of PPy thin film can be greatly improved by preparing PPy film on a functionalized partial-exfoliated graphite substrate and dope the film with β-naphthalene sulfonate anions. The flexible nature of FEG substrate accommodates large volumetric deformation of PPy during repeated charge and discharge processes. β-naphthalenesulfonate anion doping compared to the conventional SO_4^{2-} doping can better minimize the counterion drain effect and retains good electrical conductivity of PPy film. These two factors substantially enhance the cycling stability of PPy. The FEG/PPy-NS electrode exhibited outstanding capacitance retention of 97.5% after 10 000 cycles in 3 M KCl aqueous electrolyte, whereas the PPy-S and FEG/PPy-S retained only 46.8% and 82.6% of the capacitance under the same test conditions. Moreover, an asymmetric pseudocapacitor based on the stabilized FEG/PPy-NS anode showed a remarkable capacitive

Table 1. Cycling stability of PPy-based pseudocapacitor devices.

Device[a)]	Electrolyte[b)]	Current density/scan rate	Capacitance retention
V_2O_5-PPy/RGO symmetric[28]	PVA/H_2SO_4	10 [A g^{-1}]	88.1% (5000 cycles)
V_2O_5-PPy symmetric[26]	PVA/LiCl	9 [mA cm^{-2}]	80% (5000 cycles)
GF/CNTs/PPy//GF/CNTs/MnO_2[27]	0.5 M Na_2SO_4	1.5 [mA cm^{-2}]	83.5% (10 000 cycles)
PPy@MoO_3//AC[30]	0.5 M K_2SO_4	0.5 [A g^{-1}]	83% (600 cycles)
PPy-NPG//MnO_2-NPG[31]	1 M $LiClO_4$	100 [mV s^{-1}]	85% (2000 cycles)
PPy@cellulose symmetric[22]	2 M NaCl	30 [mA cm^{-2}]	84% (8500 cycles)
PPy hydrogel symmetric[32]	PVA/H_2SO_4	–[c)]	90% (3000 cycles)
PPy-MWCNT symmetric[33]	0.5 M Na_2SO_4	20 [mA cm^{-2}]	94.2% (5000 cycles)
BC/PPy/MWCNTs symmetric[34]	2 M LiCl	10 [mA cm^{-2}]	94.5% (5000 cycles)
PPy//MnO_2[29]	1 M Na_2SO_4	–[c)]	80% (2000 cycles)
WO_3@PPy//CF-Co(OH)$_2$[35]	3 M NaOH	100 [mV s^{-1}]	85% (5000 cycles)
FEG/PPy-NS//FEG/MnO_2 (This work)	3 M KCl	6 [A g^{-1}] (≈5 mA cm^{-2})	97% (10 000 cycles)

[a)]All assymmetric devices are denoted as "anode//cathode;" [b)]PVA: polyvinyl alcohol gel electrolyte; [c)]Not reported.

retention of 97% in aqueous electrolyte, which is the best value achieved for PPy-based electrochemical capacitor devices.

4. Experimental Section

Materials: All the chemicals were purchased from Sinopharm Chemical Reagent Co., Ltd. (P. R. China) and used as received except pyrrole which was used after reduced pressure distillation (≈80 kPa, 110 °C, 40 min). Cellulose separators were purchased from Nippon Kodoshi Corporation (Japan) and used as received. Graphite foils are purchased from SGL group (Germany).

Preparation of Functionalized Partial-Exfoliated Graphite Substrates (FEG) and FEG/MnO_2 Electrode: FEG substrates were prepared by a two-step exfoliation method reported elsewhere.[19] A piece of graphite foil was used as a working electrode in a three-electrode electrochemical cell with SCE reference electrode (0.2444 V versus standard hydrogen electrode) and Pt plate as counter electrode. The graphite electrode was scanned between 0.5 and 1.8 V versus SCE at 20 mV s^{-1} in 0.5 M K_2CO_3 aqueous solution (pH = 11.8) for six cycles. The electrode was then further scanned for another ten cycles in a phosphate buffered saline containing 1 M KNO_3 (pH = 6.7) between −1.0 and 1.9 V versus SCE at 20 mV s^{-1}. In each cycle, the electrode was kept at 1.9 V versus SCE for 5 s. Last, the electrode was washed with ethanol and deionized water to remove inorganic residuals on the surface. For preparing FEG supported MnO_2 electrode, MnO_2 nanosheets were deposited on the FEG substrate at a constant current density of 0.2 mA cm^{-2} for 35 min at ambient conditions in an aqueous solution containing 0.01 M manganese acetate and 0.02 M ammonium acetate.

Electropolymerization of Pyrrole: PPy film doped with β-naphthalene sulfonic anions was electrochemically deposited on FEG substrate through electropolymerization in a solution of 0.1 M pyrrole and 0.05 M β-naphthalene sulfonic acid at 2 mA cm^{-2} for 6 min. The electrode is denoted as FEG/PPy-NS. For comparison, PPy films doped with sulfate ions, a smaller anion contains the same sulfonic acid group as NS^- (Figure S1, Supporting Information), were prepared by electropolymerization on FEG (denoted as FEG/PPy-S) and graphite foils (denoted as PPy-S) in a 0.1 M pyrrole and 0.05 M H_2SO_4 aqueous solution at 2 mA cm^{-2} as control samples. After electrodeposition, the electrodes were washed with ethanol and deionized water. The mass loading was calculated based on the weight difference between the dried electrodes (vacuum dried at 60 °C for 24 h) before and after electrodeposition, using a Sartorius BT 25 S semimicrobalance with a sensitivity of 0.01 mg. The mass loadings of PPy for the aforementioned three electrodes were adjusted to the same amount (0.56 ± 0.01 mg cm^{-2}) by controlling the time of electrodeposition. PPy-S electrodes with reduced mass loading of 0.12 ± 0.01 mg cm^{-2} were produced by the same condition as PPy-S except the electrodeposition time was reduced from 15 to 2 min.

Assembly of FEG/PPy-NS//FEG/MnO_2 Asymmetric Pseudocapacitor Device: The asymmetric pseudocapacitor device was assembled using FEG/PPy-NS (working area 1 cm × 1 cm) as anode and FEG/MnO_2 (working area 1 cm × 1 cm) as cathode. The mass loading of anode (0.56 ± 0.01 mg cm^{-2}) and cathode (0.23 ± 0.01 mg cm^{-2}) were adjusted to balance the charge on both sides (calculation, Supporting Information). A piece of cellulose paper was used to separate the two electrodes.

Characterization: Morphologies of the electrodes were investigated by scanning electron microscopy (SEM, Ultra Plus, Carl Zeiss, Germany). Energy-dispersive spectroscopy (EDS, Ultra Plus, Carl Zeiss, Germany) measurements were performed to determine the elements of the synthesized electrodes. XPS measurements were performed on a XPS spectrometer (ESCALAB 250Xi, Thermo Scientific Escalab, USA) with Al K_α radiation (λ = 8.34 Å) as the excitation source. The binding energies of peaks were calibrated using the C 1s photoelectron peak at 284.6 eV as reference. Electrochemical measurements were conducted in a three-electrode electrochemical reactor using a multichannel electrochemical analyzer (VMP3, Bio-Logic-Science Instruments, France). PPy-S, FEG/PPy-S, and FEG/PPy-NS electrodes (working area: 1 cm^2) were used as working electrodes, with a Pt plate as the counter electrode and a SCE electrode as the reference electrode. Cyclic voltammetry (CV) and galvanostatic charge/discharge data were collected in 3 M KCl aqueous electrolyte. Electrochemical impedance spectroscopy (EIS) was performed at open-circuit potential from 20 kHz to 50 mHz with a perturbation of 10 mV in 3 M KCl aqueous electrolyte. Electrochemical cycling stability of the electrode and the device was tested by galvanostatic charge/discharge cycling measurements for 10 000 cycles in 3 M KCl aqueous electrolyte.

Supporting Information

Supporting Information is available from the Wiley Online Library or from the author.

Acknowledgements

Y.S. and T.-Y.L. contributed equally to this work. X.-X.L. gratefully acknowledges financial supports from National Natural Science Foundation of China (Grant No. 21273029) and Research Foundation for Doctoral Program of Higher Education of China (Grant No. 20120042110024). X.-X.X. gratefully acknowledges financial supports from National Natural Science Foundation of China (Grant No. 21303010). Y.L. acknowledges the financial support of Faculty Research Grant awarded by the Committee on Research from the University of California, Santa Cruz.

Received: April 27, 2015
Revised: May 28, 2015
Published online: June 18, 2015

[1] T. Liu, L. Finn, M. Yu, H. Wang, T. Zhai, X. Lu, Y. Tong, Y. Li, *Nano Lett.* **2014**, *14*, 2522.
[2] Y. Song, J. Xu, X. Liu, *J. Power Sources* **2014**, *249*, 48.
[3] M. Bai, T. Liu, F. Luan, Y. Li, X. Liu, *J. Mater. Chem. A* **2014**, *2*, 10882.
[4] Y. Zhao, B. Liu, L. Pan, G. Yu, *Energ. Environ. Sci.* **2013**, *6*, 2856.
[5] W. Zhang, X. Wen, S. Yang, *Langmuir* **2003**, *19*, 4420.
[6] J. Heinze, B. A. Frontana-Uribe, S. Ludwigs, *Chem. Rev.* **2010**, *110*, 4724.
[7] G. Yu, X. Xie, L. Pan, Z. Bao, Y. Cui, *Nano Energy* **2013**, *2*, 213.
[8] T. F. Otero, J. G. Martinez, *Adv. Funct. Mater.* **2013**, *23*, 404.
[9] T. F. Otero, M. Alfaro, V. Martinez, M. A. Perez, J. G. Martinez, *Adv. Funct. Mater.* **2013**, *23*, 3929.
[10] T. F. Otero, J. G. Martinez, *Adv. Funct. Mater.* **2014**, *24*, 1259.
[11] C. Meng, C. Liu, L. Chen, C. Hu, S. Fan, *Nano Lett.* **2010**, *10*, 4025.
[12] a) L.-Z. Fan, J. Maier, *Electrochem. Commun.* **2006**, *8*, 937; b) Q. Wu, Y. Xu, Z. Yao, A. Liu, G. Shi, *ACS Nano* **2010**, *4*, 1963.
[13] S. Biswas, L. T. Drzal, *Chem. Mater.* **2010**, *22*, 5667.
[14] J. Zhang, X. S. Zhao, *J. Phys. Chem. C* **2012**, *116*, 5420.
[15] K. Shi, I. Zhitomirsky, *J. Power Sources* **2013**, *240*, 42.
[16] S. Chen, I. Zhitomirsky, *J. Power Sources* **2013**, *243*, 865.
[17] a) Y. Liu, H. Wang, J. Zhou, L. Bian, E. Zhu, J. Hai, J. Tang, W. Tang, *Electrochim. Acta* **2013**, *112*, 44; b) N. O. Weiss, H. Zhou, L. Liao, Y. Liu, S. Jiang, Y. Huang, X. Duan, *Adv. Mater.* **2012**, *24*, 5782; c) F. Bonaccorso, L. Colombo, G. Yu, M. Stoller, V. Tozzini, A. C. Ferrari, R. S. Ruoff, V. Pellegrini, *Science* **2015**, *347*, 1246501.
[18] H. Fu, Z. Du, W. Zou, H. Li, C. Zhang, *J. Mater. Chem. A* **2013**, *1*, 14943.
[19] Y. Song, D. Feng, T. Liu, Y. Li, X. Liu, *Nanoscale* **2015**, *7*, 3581.
[20] M. D. Ingram, H. Staesche, K. S. Ryder, *J. Power Sources* **2004**, *129*, 107.

[21] C. Weidlich, K. M. Mangold, K. Jüttner, *Electrochim. Acta* **2005**, *50*, 1547.
[22] Z. Wang, P. Tammela, P. Zhang, M. Strømme, L. Nyholm, *J. Mater. Chem. A* **2014**, *2*, 16761.
[23] J. Zhang, P. Chen, B. H. L. Oh, M. B. Chan-Park, *Nanoscale* **2013**, *5*, 9860.
[24] H. Ge, G. Qi, E.-T. Kang, K. G. Neoh, *Polymer* **1994**, *35*, 504.
[25] a) X. Lu, M. Yu, T. Zhai, G. Wang, S. Xie, T. Liu, C. Liang, Y. Tong, Y. Li, *Nano Lett.* **2013**, *13*, 2628; b) M. Beidaghi, C. Wang, *Adv. Funct. Mater.* **2012**, *22*, 4501; c) W. Jiang, D. Yu, Q. Zhang, K. Goh, L. Wei, Y. Yong, R. Jiang, J. Wei, Y. Chen, *Adv. Funct. Mater.* **2015**, *25*, 1063; d) M. Huang, Y. Zhang, F. Li, L. Zhang, R. S. Ruoff, Z. Wen, Q. Liu, *Sci. Rep.* **2014**, *4*, 3878; e) V. Augustyn, P. Simon, B. Dunn, *Energy Environ. Sci.* **2014**, *7*, 1597.
[26] M. Bai, L. Bian, Y. Song, X. Liu, *ACS Appl. Mater. Inter.* **2014**, *7*, 12656.
[27] J. Liu, L. Zhang, H. B. Wu, J. Lin, Z. Shen, X. W. Lou, *Energy Environ. Sci.* **2014**, *7*, 3709.
[28] C. Yu, P. Ma, X. Zhou, A. Wang, T. Qian, S. Wu, Q. Chen, *ACS Appl. Mater. Inter.* **2014**, *6*, 17937.
[29] F. Grote, Y. Lei, *Nano Energy* **2014**, *10*, 63.
[30] Y. Liu, B. Zhang, Y. Yang, Z. Chang, Z. Wen, Y. Wu, *J. Mater. Chem. A* **2013**, *1*, 13582.
[31] Y. Hou, L. Chen, P. Liu, J. Kang, T. Fujita, M. Chen, *J. Mater. Chem. A* **2014**, *2*, 10910.
[32] Y. Shi, L. Pan, B. Liu, Y. Wang, Y. Cui, Z. Bao, G. Yu, *J. Mater. Chem. A* **2014**, *2*, 6086.
[33] Y. Zhu, K. Shi, I. Zhitomirsky, *J. Mater. Chem. A* **2014**, *2*, 14666.
[34] S. Li, D. Huang, J. Yang, B. Zhang, X. Zhang, G. Yang, M. Wang, Y. Shen, *Nano Energy* **2014**, *9*, 309.
[35] F. Wang, X. Zhan, Z. Cheng, Z. Wang, Q. Wang, K. Xu, M. Safdar, J. He, *Small* **2015**, *11*, 749.